

Highest Recorded N–O Stretching Frequency for 6-Coordinate {FeNO}⁷ Complexes: An Iron Nitrosyl Model for His₃ Active SitesJia Li,[†] Atanu Banerjee,[†] Piotr L. Pawlak,[†] William W. Brennessel,[‡] and Ferman A. Chavez^{*,†}[†]Department of Chemistry, Oakland University, Rochester, Michigan 48309-4477, United States[‡]Department of Chemistry, University of Rochester, Rochester, New York 14627-0216, United States

S Supporting Information

ABSTRACT: We report the synthesis, structure, and reactivity of [Fe(T1Et4iPrIP)(OTf)₂] (**1**; T1Et4iPrIP = tris(1-ethyl-4-isopropylimidazolyl)phosphine). Compound **1** reacts reversibly with nitric oxide to afford [Fe(T1Et4iPrIP)(NO)(THF)(OTf)(OTf)] (**2**), which is the first example of a 6-coordinate {FeNO}⁷ *S* = 3/2 complex containing a linear Fe–N–O group. **2** exhibits the highest $\nu(\text{NO})$ for compounds in this class. Density functional theory studies reveal an enhanced degree of β -electron transfer from $\pi^*(\text{NO})$ to the Fe *d* orbitals accounting for the large stretching frequency.

Class III nonheme dioxygenases possess iron(II) coordination sites bearing three histidine residues, which contrasts with Class I and II sites containing 2His-1-carboxylate metal binding sites. The lack of a carboxylate group in the first coordination sphere renders the iron site more Lewis acidic by altering the mechanism for dioxygenase reactivity. Enzymes containing His₃ metal binding sites include gentisate 1,2-dioxygenase, salicylate 1,2-dioxygenase, 3-hydroxyanthranilate 3,4-dioxygenase, 1-hydroxy-2-naphthoate dioxygenase, and cysteine dioxygenase.¹ These enzymes belong to the cupin superfamily characterized by two highly conservative sequence motifs of G(X)₅HXH(X)_{3,4}E(X)₆G and G(X)₅PXG(X)₂H(X)₃N.² Nitric oxide has been used to characterize ferrous active sites because they are electron paramagnetic resonance (EPR) silent and do not exhibit low-energy absorption bands.³ Although many nonheme enzymes form stable Fe–NO complexes, a number of them are known to react reversibly^{3a} with the formation of paramagnetic nitrosyl iron centers, which according to the Enemark and Feltham notation are of the {FeNO}⁷ type.⁵ These nonheme iron enzyme nitrosyl derivatives invariably possess an EPR-active *S* = 3/2 ground state characterized by an axial EPR spectrum with *g*_x, *g*_y, and *g*_z values of ~4, ~4, and ~2, respectively. Researchers have used Raman, magnetic circular dichroism, EPR, Mössbauer spectroscopies, SCF-*X* α -SW, and generalized gradient approximation (GGA) density functional theory (DFT) calculations and have determined that these {FeNO}⁷ (*S* = 3/2) species are the result of high-spin ferric (*S* = 5/2) antiferromagnetically coupled to NO⁻ (*S* = 1).^{3b,6} The acquisition of synthetic complexes capable of reversibly binding NO is an important aspect for accurately modeling these enzymes. In our efforts to synthesize models that reproduce the reversibility of iron nitrosyl formation, we have employed the ligand tris(1-ethyl-4-isopropylimidazolyl)phosphine (T1Et4i-

PrIP).⁷ The reaction of T1Et4iPrIP with Fe(OTf)₂·2MeCN affords [Fe(T1Et4iPrIP)(OTf)₂] (**1**; Figure 1). In the structure

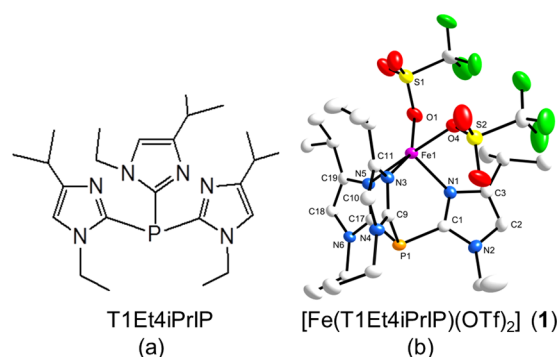


Figure 1. (a) T1Et4iPrIP and (b) a thermal ellipsoid plot (50% probability) for **1**. H atoms have been omitted for clarity.

of **1**, iron(II) is bonded to three imidazole N atoms in a facial manner along with two O atoms from the triflates to afford highly distorted trigonal-bipyramidal geometry ($\tau = 0.33$)⁸ with one O atom and one N atom occupying the apical positions.

The reaction of a colorless solution of **1** in tetrahydrofuran (THF) with nitric oxide at 25 °C yields a yellow-brown solution (Figure S1 in the Supporting Information, SI). The three-band pattern in the UV–vis spectrum, with relatively intense absorption features in the near-UV region, followed by an absorption band with intermediate intensity in the 400–500 nm region and a weaker absorption band between the 600 and 700 nm region is characteristic of iron nitrosyl compounds.⁹ The band centered at ~455 nm is assigned to a Fe–NO metal-to-ligand charge-transfer band. When a vacuum is applied to the reaction mixture or argon is bubbled into the solution, the band near 455 nm diminishes, giving a spectrum similar to that of the starting material. This process is reversible over several cycles.

The crystal structure for the nitrosyl adduct reveals a bound NO molecule along with a coordinated THF and triflate group. The asymmetric unit cell contains two iron cations and two triflate groups. One of the cations (Figure 2) shows a slightly bent Fe–N–O unit with an angle of 168.6(5)° and Fe–NO and N–O distances of 1.765(5) and 1.146(6) Å, respectively, while the other exhibits a more linear Fe–N–O unit with an angle of 174.4(4)°, a Fe–NO distance of 1.763(5) Å, and a N–O

Received: March 17, 2014

Published: May 19, 2014

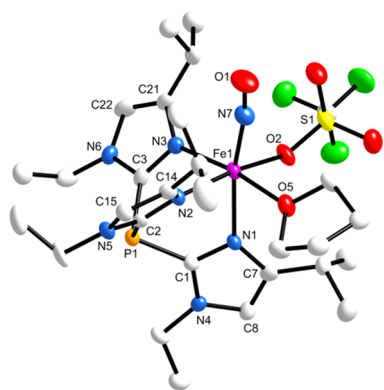


Figure 2. Thermal ellipsoid plot (50% probability) for $[\text{Fe}(\text{T1Et4iPrIP})(\text{THF})(\text{OTf})(\text{NO})]^+$ (cation of **2**). H atoms have been omitted for clarity.

distance of 1.153(6) Å. The observed Fe–N–O angles can mostly be ascribed to electronic and not steric effects because the nearest interaction between the O atom of NO and the ligand is 3.174 Å (O1–C12). Having Fe–N–O angles greater than 165° constitutes **2** as the first example of a linear FeNO complex in this class.¹⁰

The EPR spectrum for **2** in toluene/THF glass at 77 K shows $S = 3/2$ signals with effective g values of 3.90 and 2.01 (Figure S2 in the SI). These data are in accordance with the well-established electronic structure of nonheme ferrous nitrosyls, which show $\text{Fe}^{\text{III}}\text{--NO}^-$ ground states where the high-spin Fe^{III} and NO^- ($S = 1$) are antiferromagnetically coupled.^{3b} The high concentration (20 mM) needed to achieve a good signal suggests a low concentration of this species, however.

Although **2** is relatively stable in a THF/pentane solution at 25 °C under an atmosphere of NO, Park et al.¹¹ observed that $[\text{Fe}(\text{PhTIP})(\text{acac})(\text{NO})]$ [PhTIP = tris(2-phenylimidazol-4-yl)phosphine] was only moderately stable at –40 °C in MeCN. The difference in the nitrosyl-adduct stability could be due to either the higher steric shielding and/or greater electron-withdrawing nature of the 4-phenyl groups on PhTIP or the lack of a 1-alkyl group on the imidazole ring (compared to T1Et4iPrIP). Like **2**, $[\text{Fe}(\text{6TLA})(\text{BF})(\text{ClO}_4)]^{\text{9a}}$ {6TLA = tris[(6-methyl-2-pyridyl)methyl]amine; BF = benzoylformate} reversibly binds NO to afford the nitrosyl adduct $[\text{Fe}(\text{6TLA})(\text{BF})(\text{NO})(\text{ClO}_4)]$.

Vibrational spectroscopy was used to further characterize the nature of the Fe–NO unit in **2** (Figure S3 in the SI). Importantly, the IR spectra of **2** (KBr) exhibits a $\nu(\text{NO})$ stretching frequency, which is the highest (1831 cm^{-1}) observed for 6-coordinate iron(II) nitrosyl complexes with $\{\text{FeNO}\}^7$ (Figure 3 and Table S1 in the SI), occurring only 44 cm^{-1} below the stretching vibration of free NO (1875 cm^{-1}).¹² When the spectrum is taken in a THF solution, we observe a value of 1820 cm^{-1} , suggesting that crystal packing may have some influence on the solid-state value.

There is a positive correlation between the Fe–N–O bond angle for 6-coordinate $\{\text{FeNO}\}^7$ complexes and $\nu(\text{NO})$ (Figure 3).^{3b,9a,13–20} The average Fe–N–O angle (171.5°) for **2** is used in this plot. Such a correlation was previously observed for 5-coordinate $\{\text{FeNO}\}^7$ complexes.¹⁵ The correlation is particularly strong when compounds exhibiting spin-crossover^{15,22} and close contacts between the coordinated NO and other ligands^{6a,21} are excluded.

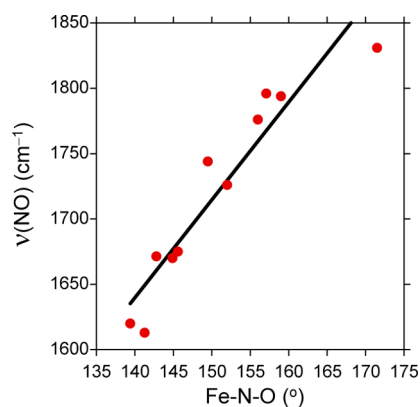


Figure 3. Plot of the Fe–N–O angle versus $\nu(\text{NO})$ for 6-coordinate $\{\text{FeNO}\}^7$ compounds (linear fit, $R = 0.95$).^{3b,9a,13–20}

In a study of 5-coordinate complexes,²³ the relationship seen in Figure 3 was reversed. One explanation for this could be that the observed Fe–N–O angle was not under electronic but steric control. The interaction between the NO group and ligand substituents could influence $\nu(\text{NO})$, thus masking the correlation. It can be seen that the least influenced NO ligand in this study along with a recent example²⁴ correlates well with the previously mentioned study.¹⁵

DFT calculations have previously been performed on FeNO compounds.^{9b,24} The PBE0 6-31+G*-optimized structure on the cation of **2** shows excellent agreement with experimental values. The Fe–NO distances of 1.765 and 1.789 Å are only slightly smaller than the calculated value of 1.795 Å. Fe–N–O angles of 164.5 and 174.4° are very close to the calculated value of 173.24°. The N–O bond distances of 1.146 and 1.153 Å (calcd: 1.157 Å) also compare well. Most importantly, the calculated N–O stretching frequency of 1839 cm^{-1} (scale factor = 0.938) is very close to the experimental (KBr) value (1831 cm^{-1}). Thus, the DFT results essentially reproduce the experimental metric and vibrational values. Analysis of the molecular orbital (MO) diagram demonstrates an electronic-structural description that is consistent with the high-spin $\text{Fe}^{\text{III}}\text{--NO}^-$ bonding scheme.^{3b} Correspondingly, in the α -spin MO diagrams, all of the Fe d orbitals are (singly) occupied. In the applied coordinate system (Fe–NO vector corresponding to the z axis), the d_{xz} and d_{yz} orbitals do not participate in back-bonding with the two unoccupied $\alpha\text{-}\pi^*$ orbitals of NO.

In the β -spin MO diagram, all of the Fe d orbitals are empty, whereas the $\beta\text{-}\pi^*$ orbitals of NO are occupied. These occupied orbitals are situated to donate into the empty β -spin d_{xz} and d_{yz} orbitals of Fe. The strength of this interaction can be estimated from the corresponding antibonding combinations $\beta 193$ (42% d_{yz} , 58% π^*) and $\beta 194$ (38% d_{xz} , 62% π^*) for the cation of **2**, which show significant Fe d orbital and NO π^* character (see Figure 4). As a result, the π donation from NO^- is significant. This result was also observed in $[\text{Fe}(\text{BMPA-Pr})\text{Cl}(\text{NO})]$.¹³

The calculated spin-density values for Fe and NO are +3.93 and –1.15, respectively. These values reflect the strong donation of negative (β) spin density from NO to Fe, rendering NO to appear closer to NO^\bullet and Fe closer to Fe^{2+} . Because the donation originates from N–O π^* orbitals, a strengthening of this interaction should result in a strengthening of the N–O bond and a corresponding increase in the N–O stretch. The description of NO as closer to that of NO^\bullet could account for the greater reactivity compared to that of $[\text{Fe}(\text{BMPA-Pr})\text{Cl}(\text{NO})]$. Additionally, Lehnert and co-workers observed that

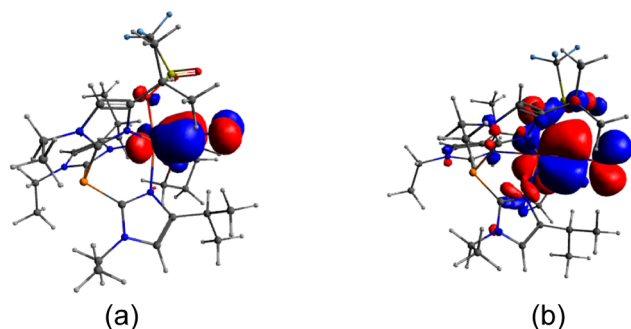


Figure 4. β -spin isosurface plots for Fe d orbitals and π^* orbitals of NO for the cation of **2**: (a) β 193 (Fe 42%, NO 58%); (b) β 194 (Fe 42%, NO 58%).

decreasing the negative charge on the iron center results in increasing the iron's ability to accept electron donation from bound NO^- .¹³ Unlike $[\text{Fe}(\text{BMPA-Pr})\text{Cl}(\text{NO})]$, we do not observe back-bonding between Fe α - d_{z^2} and α - π^* of NO^- because of the near-linearity of the Fe–N–O bond in **2**. The lack of α -spin donation from Fe to NO could also account for the long Fe–NO bond distance.

In summary, we have synthesized an accurate model for His₃ enzymes. The model reversibly binds nitric oxide to generate a 6-coordinate $\{\text{FeNO}\}^7$ iron nitrosyl species with a nearly linear Fe–N–O bond angle. The $\nu(\text{NO})$ stretching vibration is the highest recorded to date, and a strong correlation between the Fe–N–O bond angle and $\nu(\text{NO})$ is observed when these parameters are plotted for other known 6-coordinate $\{\text{FeNO}\}^7$ complexes. Computational studies indicate that the bonding in the nitrosyl group can be described as a high-spin Fe^{III} ($S = 5/2$) antiferromagnetically coupled to NO^- ($S = 1$), where the Fe–NO bond consists mostly of β electrons being donated back to the iron center. This accounts for the high N–O vibrational frequency.

■ ASSOCIATED CONTENT

Supporting Information

Experimental materials, methods, and figures along with crystallographic information (CIF). This material is available free of charge via the Internet at <http://pubs.acs.org>.

■ AUTHOR INFORMATION

Corresponding Author

*E-mail: chavez@oakland.edu.

Notes

The authors declare no competing financial interest.

■ ACKNOWLEDGMENTS

We thank Prof. M. D. Sevilla for assistance with EPR. We thank Dr. V. G. Young, Jr. for X-ray structure determination of **1**. We thank Prof. M. M. Szczeniński for assistance with the DFT calculations. National Science Foundation (NSF) Grant CHE-0748607 is gratefully acknowledged. An NSF award (Grant CHE-0821487) is also acknowledged.

■ REFERENCES

(1) (a) Buongiorno, D.; Straganz, G. D. *Coord. Chem. Rev.* **2013**, *257*, 541. (b) Chavez, F. A.; Banerjee, A.; Sljivic, B. Modeling the Metal Binding Site in Cupin Proteins. In *On Biomimetics*; Pramatarova, L. D., Ed.; InTech: Rijeka, Croatia, 2011.

(2) Dunwell, J. M.; Culham, A.; Carter, C. E.; Sosa-Aguirre, C. R.; Goodenough, P. W. *Trends Biochem. Sci.* **2001**, *26*, 740.

(3) (a) Orville, A. M.; Chen, V. J.; Krauciunas, A.; Harpel, M. R.; Fox, B. G.; Münck, E.; Lipscomb, J. D. *Biochemistry* **1992**, *31*, 4602. (b) Brown, C. A.; Pavlosky, M. A.; Westre, T. E.; Zhang, Y.; Hedman, B.; Hodgson, K. O.; Solomon, E. I. *J. Am. Chem. Soc.* **1995**, *117*, 715.

(4) (a) Arciero, D. M.; Lipscomb, J. D.; Huynh, B. H.; Kent, T. A.; Munck, E. *J. Biol. Chem.* **1983**, *258*, 4981. (b) Nocek, J. M.; Kurtz, D. M.; Sage, J. T.; Xia, Y. M.; Debrunner, P.; Shiemke, A. K.; Sandersloehr, J.; Loehr, T. M. *Biochemistry* **1988**, *27*, 1014. (c) Rodriguez, J. H.; Xia, Y. M.; Debrunner, P. G. *J. Am. Chem. Soc.* **1999**, *121*, 7846. (d) Haskin, C. J.; Ravi, N.; Lynch, J. B.; Münck, E.; Que, L. *Biochemistry* **1995**, *34*, 11090. (e) Chen, V. J.; Orville, A. M.; Harpel, M. R.; Frolik, C. A.; Surerus, K. K.; Münck, E.; Lipscomb, J. D. *J. Biol. Chem.* **1989**, *264*, 21677.

(5) Enemark, J. H.; Feltham, R. D. *Coord. Chem. Rev.* **1974**, *13*, 339.

(6) (a) Hauser, C.; Glaser, T.; Bill, E.; Weyhermüller, T.; Wieghardt, K. *J. Am. Chem. Soc.* **2000**, *122*, 4352. (b) Westre, T. E.; Diccico, A.; Filipponi, A.; Natoli, C. R.; Hedman, B.; Solomon, E. I.; Hodgson, K. O. *J. Am. Chem. Soc.* **1994**, *116*, 6757.

(7) Lynch, W. E.; Kurtz, D. M., Jr.; Wang, S.; Scott, R. A. *J. Am. Chem. Soc.* **1994**, *116*, 11030.

(8) Addison, A. W.; Rao, T. N.; Reedijk, J.; van Rijn, J.; Verschoor, G. C. *J. Chem. Soc., Dalton Trans.* **1984**, 1349.

(9) (a) Chiou, Y. M.; Que, L. *Inorg. Chem.* **1995**, *34*, 3270. (b) Berto, T. C.; Speelman, A. L.; Zheng, S.; Lehnert, N. *Coord. Chem. Rev.* **2013**, *257*, 244.

(10) McCleverty, J. A. *Chem. Rev.* **2004**, *104*, 403.

(11) Park, H.; Bittner, M. M.; Baus, J. S.; Lindeman, S. V.; Fiedler, A. T. *Inorg. Chem.* **2012**, *51*, 10279.

(12) Richter-Addo, G. B.; Legzdins, P. *Metal Nitrosyls*; Oxford University Press: New York, 1992.

(13) Berto, T. C.; Hoffman, M. B.; Murata, Y.; Landenberger, K. B.; Alp, E. E.; Zhao, J. Y.; Lehnert, N. *J. Am. Chem. Soc.* **2011**, *133*, 16714.

(14) Randall, C. R.; Zang, Y.; True, A. E.; Que, L.; Charnock, J. M.; Garner, C. D.; Fujishima, Y.; Schofield, C. J.; Baldwin, J. E. *Biochemistry* **1993**, *32*, 6664.

(15) Weber, B.; Gorls, H.; Rudolph, M.; Jäger, E. G. *Inorg. Chim. Acta* **2002**, *337*, 247.

(16) Rose, M. J.; Patra, A. K.; Olmstead, M. M.; Mascharak, P. K. *Inorg. Chim. Acta* **2010**, *363*, 2715.

(17) Nebe, T.; Beitat, A.; Wurtele, C.; Ducker-Benfer, C.; van Eldik, R.; McKenzie, C. J.; Schindler, S. *Dalton Trans.* **2010**, *39*, 7768.

(18) McQuilken, A. C.; Ha, Y.; Sutherlin, K. D.; Siegler, M. A.; Hodgson, K. O.; Hedman, B.; Solomon, E. I.; Jameson, G. N.; Goldberg, D. P. *J. Am. Chem. Soc.* **2013**, *135*, 14024.

(19) Lopez, J. P.; Heinemann, F. W.; Prakash, R.; Hess, B. A.; Horner, O.; Jeandey, C.; Oddou, J. L.; Latour, J. M.; Grohmann, A. *Chem.—Eur. J.* **2002**, *8*, 5709.

(20) Patra, A. K.; Rowland, J. M.; Marlin, D. S.; Bill, E.; Olmstead, M. M.; Mascharak, P. K. *Inorg. Chem.* **2003**, *42*, 6812.

(21) Pohl, K.; Wieghardt, K.; Nuber, B.; Weiss, J. *J. Chem. Soc., Dalton Trans.* **1987**, 187.

(22) Li, M.; Bonnet, D.; Bill, E.; Neese, F.; Weyhermüller, T.; Blum, N.; Sellmann, D.; Wieghardt, K. *Inorg. Chem.* **2002**, *41*, 3444.

(23) Ray, M.; Golombek, A. P.; Hendrich, M. P.; Yap, G. P. A.; Liable-Sands, L. M.; Rheingold, A. L.; Borovik, A. S. *Inorg. Chem.* **1999**, *38*, 3110.

(24) Speelman, A. L.; Lehnert, N. *Angew. Chem., Int. Ed.* **2013**, *52*, 12283.